Supplementary Information (SI) for Analytical Methods.

Supplemental Information

3D-Printed Accessories for Nano/Microelectrodes

Cody W. Leasor, Kelly L. Vernon, Yunong Wang, Reed E. Baker and Lane A. Baker*

Department of Chemistry, Texas A&M University, 580 Ross St, College Station, TX 77843 USA

***Corresponding author:**

Lane A. Baker

(979) 845-4721; (979) 458-9829 (fax);

E-mail: lane.baker@tamu.edu

Table of Contents:

S1. CHITUBOX & PREFORM 3D printing

1. Arrangement of Electrode Holder Bodies on Build Plate

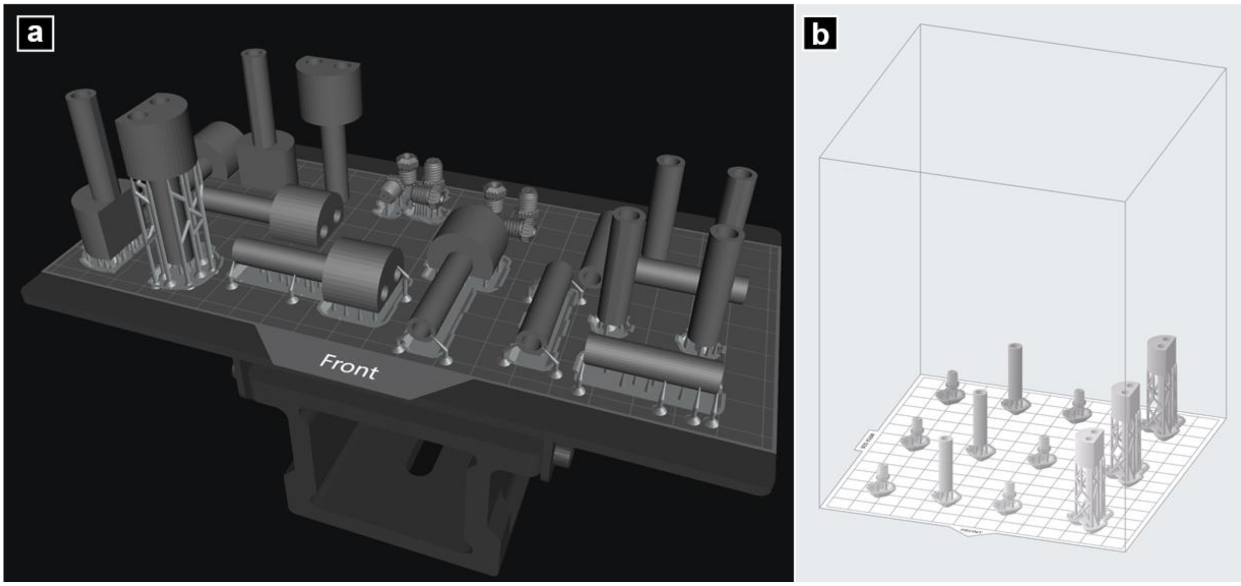

Figure S1: CHITUBOX & PREFORM 3D printing. The images displayed here is are screenshot of the CHITUBOX software (a) and PREFORM software (b) that show examples of how the electrode holder bodies and bolts were printed. For (a) there are a total number of 24 parts on the build platform, this was done because it was unknown under which orientation the individual parts would print best, so four orientations for each part was set up on the build platform which brings the sub-total number of printed parts to a dozen. The other dozen came from not knowing if it would be best to have support structures when printing the pieces or not, as a result all parts and their respective orientations were copied (bring the total to 24), where half were set up with support structures and the other half was not. It should be noted that most of the holder bodies do not show threads in this image. Threads were successfully printed in both the bolt that holds the pipettes and the bodies, however, if threads wore out or did not print correctly, a set of M5 taps and dies (with oil) were used to re-thread the parts and if necessary uncured resin was painted onto the damaged threads and cured before re-threading the parts. It was found that the orientation that works the best had support structures and the parts that were vertical aligned for both the holder bodies and the bolts. The non-supported parts had flat edges where there should have been round geometries or through-holes that were sealed due to the first few layers printing a small platform for the bodies to be printed from (requiring extra touch up maintenance that often left the part deformed or damaged). Tables S1 and S2 below, summarize the print parameters for this software used the make all the 3D prints out of Phrozen's Aqua Clear resin. For (b) there are a total number of 12 parts on the build platform, unlike (a), the orientations needed for the prints to successfully be produced were assumed to be the same as those found in (a). Similarly, all parts utilized supports to prevent damage of the printed parts as these prints were more brittle and thus more susceptible to breaking when removing them from the build platform if they do not have supports. Table S3 below, summarize the print parameters for this software used to make all of the 3D prints out of Formlabs' Rigid 10K resin.

2. Settings: Resin and Support Structures

Table S1: CHITUBOX Resin Settings

CHITUBOX Settings: *Resin*	
parameter	*setting*
layer height (mm)	0.01
bottom layer count	6
exposure time (s)	10.6
bottom exposure time (s)	35
transition layer count	6
transition type	linear
transition layer interval time difference (s)	3.49
waiting mode during printing	resting time
rest time before lift (s)	0
rest time after lift (s)	0
rest time after retract (s)	5
bottom lift distance (mm)	6
lifting distance (mm)	6
bottom lift speed (mm/min)	45
lift speed (mm/min)	45
bottom retract speed (mm/min)	150
retract speed (mm/min)	150

Table S2: CHITUBOX Support Structures' Settings

CHITUBOX Settings: *Supports*		
section	*parameter*	*setting*
basic	support type	light
	tip upper diameter (mm)	0.2
	raft shape	skate
	touch tip diameter (mm)	4
	support angle (°)	90
top*	touch shape	none
	contact depth (mm)	1
	connection shape	cone
	tip upper diameter (mm)	0.2
	tip down diameter (mm)	1
	connection length (mm)	4.5
middle*	shape	cylinder
	diameter (mm)	1
	angle (°)	45
	small pillar shape	cone
	diameter (mm)	0.1
	upper depth (mm)	5
	lower depth (mm)	5
	max. XY cross structure spacing (mm)	15
	cross start height (mm)	10
bottom*	platform touch shape	cylinder
	touch diameter (mm)	6
	thickness (mm)	1
	model contact shape	none
	contact diameter (mm)	0.2
	contact depth (mm)	0.1
	contact point	1
raft*	raft shape	skate
	raft area ratio (%)	100
	raft thickness (mm)	0.5
	raft height (mm)	1.8
	raft slope (°)	45
	grid side length (mm)	2
	grid width (mm)	2

**located in advanced settings*

Table S3: PREFORM Settings

PREFORM Settings: *Resin & Supports*		
section	*parameter*	*setting*
size	scale	1.000
	X (single-barrel)	13.75 mm
	Y (single barrel)	14.56 mm
	Z (single barrel)	32.50 mm
	X (theta barrel)	20.20 mm
	Y (theta barrel)	23.14 mm
	Z (theta barrel)	44.90 mm
	X (screw cap)	13.41 mm
	Y (screw cap)	13.31 mm
	Z (screw cap)	15.00 mm
standard workspace	printer type	Form2
	resin	Rigid 10K V1
	layer thickness	0.050 mm
	print time	5 h 46 m
	layers	833
	volume	15.11 mL
supports*	raft type (labelled)	Full Raft
	density	0.50
	touchpoint size	0.50 mm

**auto-generated supports with unchanged advanced settings*

3. Relative Cost of 3D Printers/Resins and Coefficient of Thermal Expansion

Table S4: Relative Cost and Reported Resin Mechanical Properties

Brand	*3D Printer*		*Resin*		
	Name	*Cost*	*Name*	*Cost*	*CTE* (10^{-6}/°C)*
Formlabs	Form2	$3,499.00	Rigid 10K	$299.00/L	41
Elegoo	Saturn 4 Ultra	$399.00	Tough Resin	$32.99/kg	not listed
Phrozen	Sonic Mini 8K	$379.99	Aqua Clear	$31.99/kg	not listed
			Onyx Impact Plus	$95.00/kg	not listed
Anycubic	Photon Mono M7	$299.00	Tough Resin 2.0	$35.99/kg	not listed
Stratasys	SLA Neo	$100k+	Somos PerFORM	$440/kg	49.4

**coefficient of thermal expansion*

S2. Discoloration due to Prolong U. V. light Exposure

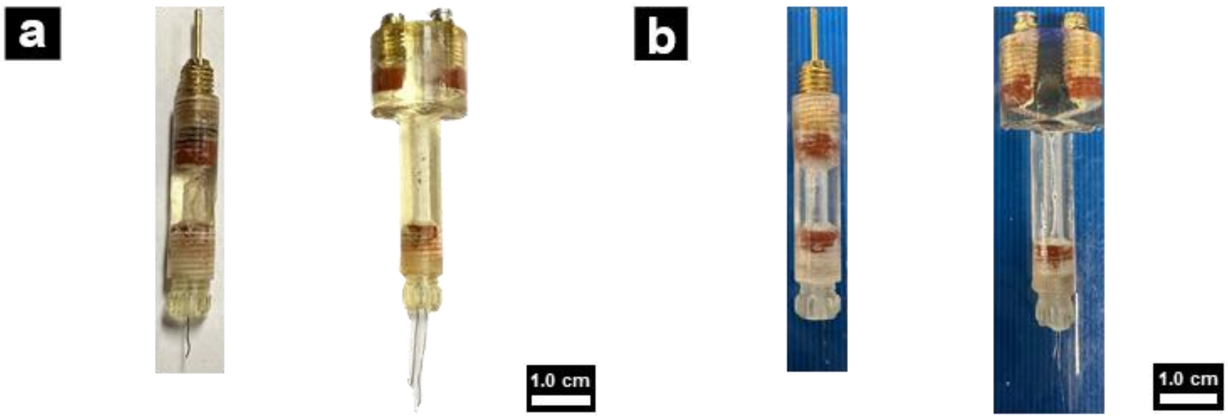

Figure S2: Discoloration due to prolonged U.V. light exposure. (a) shows a collection of two images, one for the single barrel electrode holder (left) and the theta barrel electrode holder (right) where the four printed bodies have less discoloration (less yellow tint) when exposed to a minimal U.V. light exposure (10-minute maximum). (b) shows the same as (a) for the another set of the 3D printed bodies that were exposed to 60 minutes of U.V. light. The prints in both (a) and (b) had new resin painted onto the outside of the bodies and was cured for 5-minutes to aid in their transparency, however, the extra resin did not add to the discoloration only the amount of time the parts were exposed to the U.V. light during the post curing process. As a result, it should be noted that the prints accuracy could be enhanced by prolonging the print time by making smaller vertical steps when constructing the parts layer by layer, however, this also in turn forces the previous sets of layers to be exposed to U.V. light for longer times when constructing the prints which in turn can cause uncured resin discoloration (forcing all future prints from this reservoir to be discolored) and/or partially cure small features within the uncured resin reservoir.

S3. SOLIDWORKS Design Drawings of 3D Printed Bodies

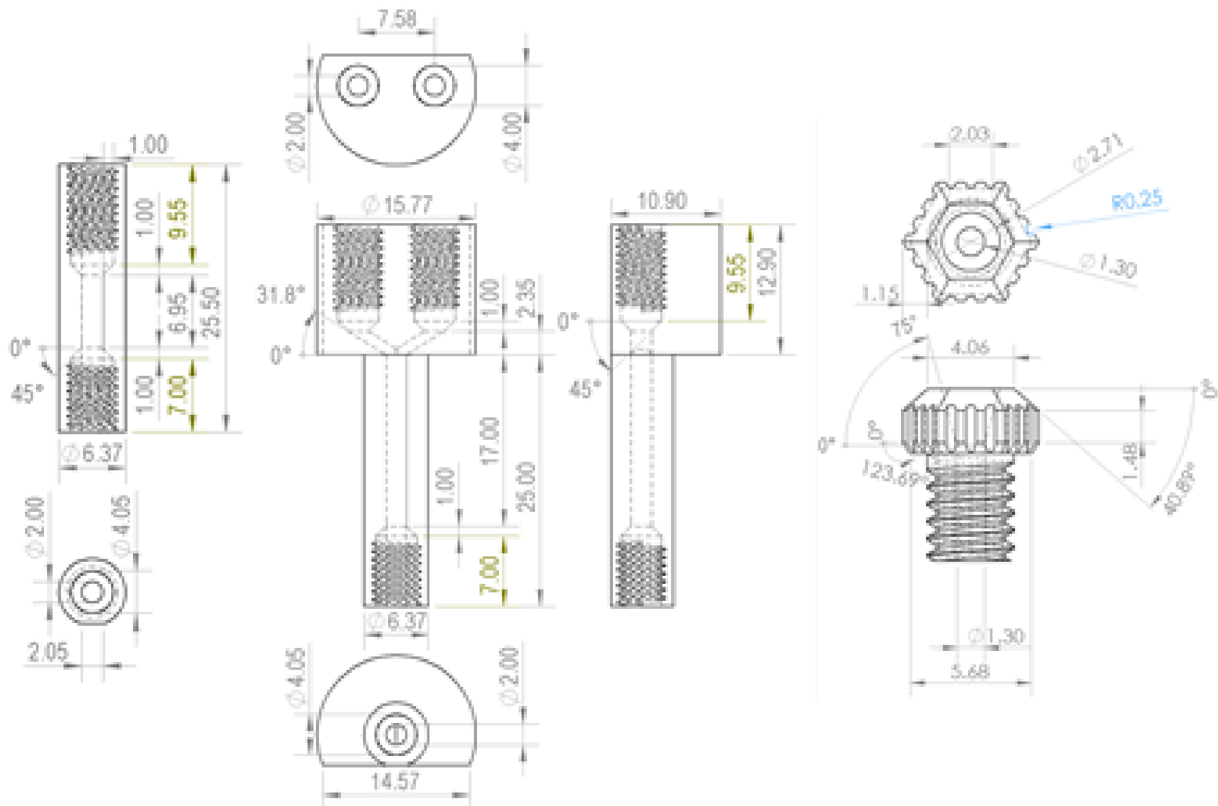

Figure S3: SOLIDWORKS design drawings of 3D printed bodies. Presented here are all the drawings were made in SOLIDWORKS with the dimension in units of mm to allow anyone to recreate these parts as necessary. The single barrel electrode body is shown on far-left side of the image and right below that body is an orthogonal view of end of the body which appears identical to the opposite end-on view (as a result this extra view was not added due to redundancy). The set of bodies in the middle of the image are representing the theta barrel electrode holder body. The middle right image is the side-view from this perspective, whereas the small body above is the top view of the body (highlighting where the bolts would be inserted) and the body below shows the bottom view (highlighting where the bolt that holds the pipette would be inserted). The right most body is the bolt that holds the pipette and above it is the top view (bottom view not shown due to redundant information).

S4. Extra Fabricated or Machined Parts

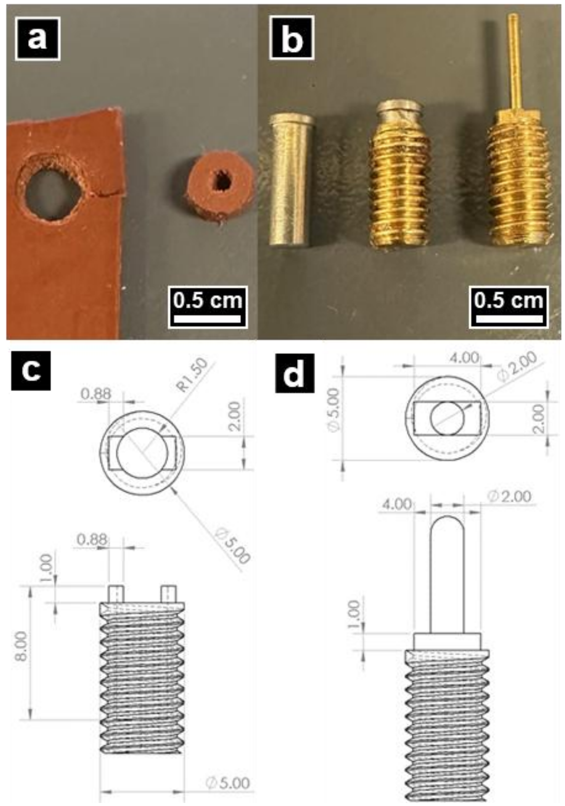

Figure S4: Extra fabricated or machined parts. (a) shows a corner of the silicone rubber sheet, used to make the gasket seals, with a 3 – 4 mm diameter hole punched out of it. Next to the sheet, is the punched cylinder that had a ca. 1.2 mm hole drilled through the center, which exemplifies how the gaskets were fabricated from the rubber sheet. (b) shows the micro-jack that was purchased (left), the machined bolt with a hole drilled into its center, with a micro-jack soldered into the hole (middle), and the machined bolt with a pin extruding from its center (right). (c) and (d) are the SOLIDWORKS drawings with dimensions in units of mm for both bolt type: with a hole and with a pin, respectively. Please note that in (c) there was supposed to be a 1 mm extrusion coming from the top of the bolt that is not seen in (b). This is due to when soldering, cleaning up (removing extra material) and trying to assemble the bolt into the holder, caused this to wear down or was purposefully removed by grinding more of the top threads down to allow for proper gripping when assembling bolt into the holder; The pin design did not require an extra solder piece to be added and as a result, no extra cleaning or grinding was needed and as a solid rectangle protruding from the top of the bolt, made it less fragile than the other design's protruding shape. All threads for the bolts and holders were printed or machined to be an M5 size.

S5. Ion Current Rectification Ratio and its Deviation from Unity

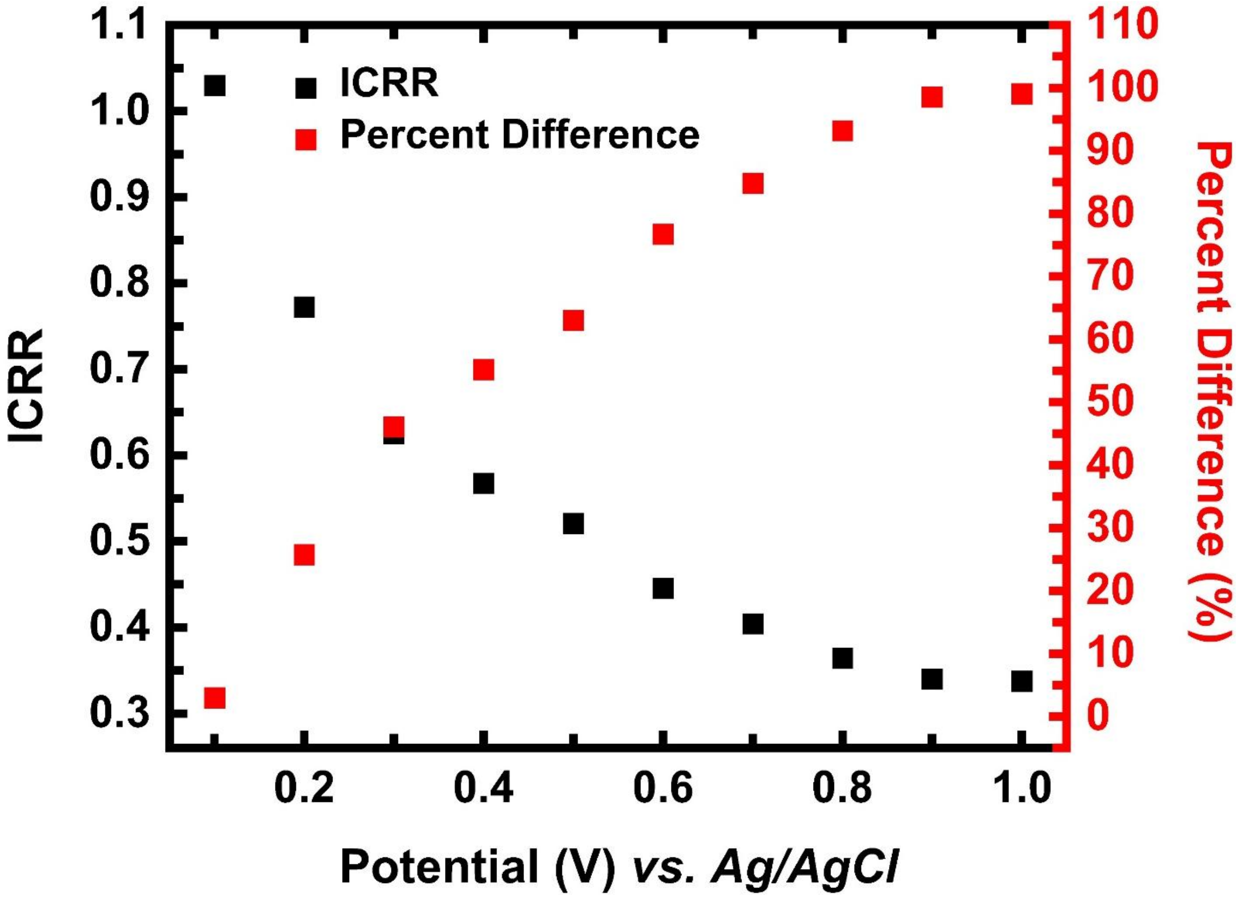

Figure S5: Overlaid plot of the grand average Ion Current Rectification Ratio (ICRR) and the percent difference from unity as a function of absolute potential vs Ag/AgCl. The ICRR was calculated from I-V curve shown in **Figure 3** and from the equation below.

$$\text{ICRR} = \left|\frac{I_{+V}}{I_{-V}}\right|$$

Where I_{+V} and I_{-V} are the measured current values at a given positive applied potential and negative potential, respectively.[1] At ±0.1 V the percent difference from unity is 3% and an ICRR value of 1.03. A point of discussion regarding the ICRR value being greater than 1 at ±0.1 V, is due to variance within the measurements and nanopipettes types as well as the individual types variance in size. Overall, the percent difference is relatively low and the vast majority of the rectification appears to be minimized at this potential, that aid in the justification for these points to be used when estimated the nanopipette tip sizes.

S6. Processing SICM Topographical Data

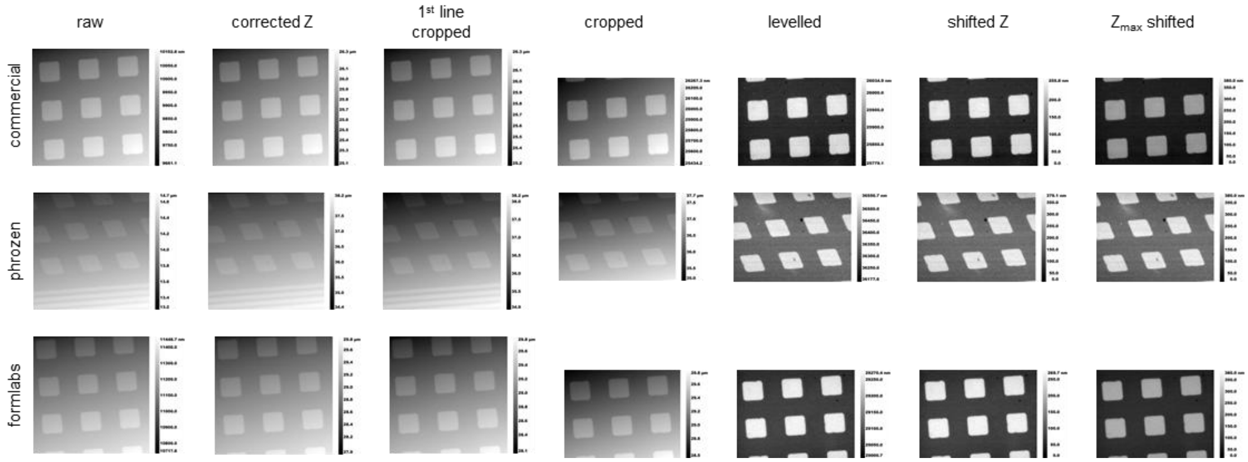

Figure S6: Processing SICM Topography Data. The array of topography maps here are only 3 sets of data, separated by the type of holder used to obtain the row of maps as the commercial, Phrozen and Formlabs electrode holders as the first, second and third rows, respectively. The columns are separated by how the data was processed. The first column is the raw data for each image, then Z axis was corrected by multiplying the values by a coefficient of 2.6 (correction factor for the piezo used) in the second column. The third column crops and removes the first line that was scanned (top line of each image) because this data does not represent part of the scan and instead is imaging the same point without changing the x or y position to calibrate the piezo response. The fourth column crops the previous image by isolating the minimum number of fully imaged features (Phrozen had the least of 5 seen in this column), which resulted in a 120 pixels x 90 pixels scan area for all of the image but at cropping origin of 0 pixel count x 3 pixel count (top left of image) for the Phrozen column and an origin of 0 pixel count x 29 pixel count for the Formlabs and commercial columns. This was followed by and shown in the next column, by leveling the data by mean plane subtraction, the next column then shifted the Z values by subtracting all of the Z values by each map's minimum Z value. Finally, the color scale was shifted such that the maximum Z value seen was 380 nm, which only changed the contrast/brightness of the images, shown in the last column.

S7. Resistance as a Function of Pipette Geometry

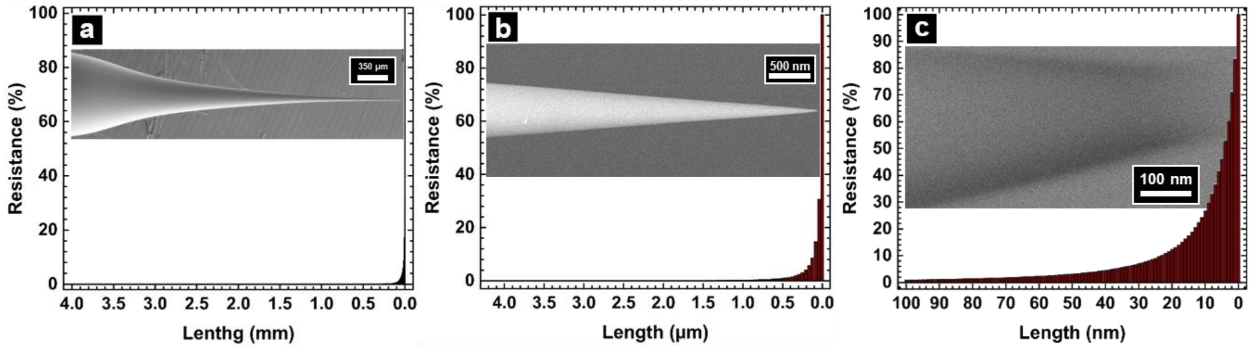

Figure S7: Resistance as a function of pipette geometry. (a) shows an inset scanning electron micrograph of a single barrel pipette that is inside of a bar chart that displays the resistance as a function of distance from the pipette tip. The resistance is normalized by taking the calculated value (see equations below) as a percent of the total resistance of the pipette, which was done for each interval distance from the tip to the length of the pipette shoulder. (b) is the same as (a) but the length considered is 4 µm from the tip. (c) is the same as (a) and (b) but with a length of 100 nm from the tip. The data displayed here as bar plots are from a python script that simulates the probe geometry and calculates the resistance from each pre-set thickness at this geometry. First the data was measured from the inset SEM image in (a), in ImageJ Fiji software to determine the X-, Y- coordinates of the tapering geometry. Next a function was obtain based on these values with a 60-degree polynomial fit such that the sum of the squared residuals was minimized. The coefficients were extracted and the inner probe radius was calculated from this equation at 1 nm length intervals. These radii were then converted to the resistance by integrating the area under two consecutive points (separated by 1 nm) and multiplying the integrand the inverse product of the solution's conductivity and the constant π. Next the sum of all resistances was taken as the reference when normalizing all sub-resistance values. Data in (a) shows the overwhelming majority of the resistance contributions come from the area at or near pipette tip orifice that is less than 0.5 mm from the tip. Data in (b) shows yet again, the majority comes from an area even closer to the tip that is less than 1 µm. Data in (c) shows this even further by showing the top 75% of the resistance occurs at or less than 10 nm away from the pipette tip orifice.

S8. Optical Microscopy Micrographs

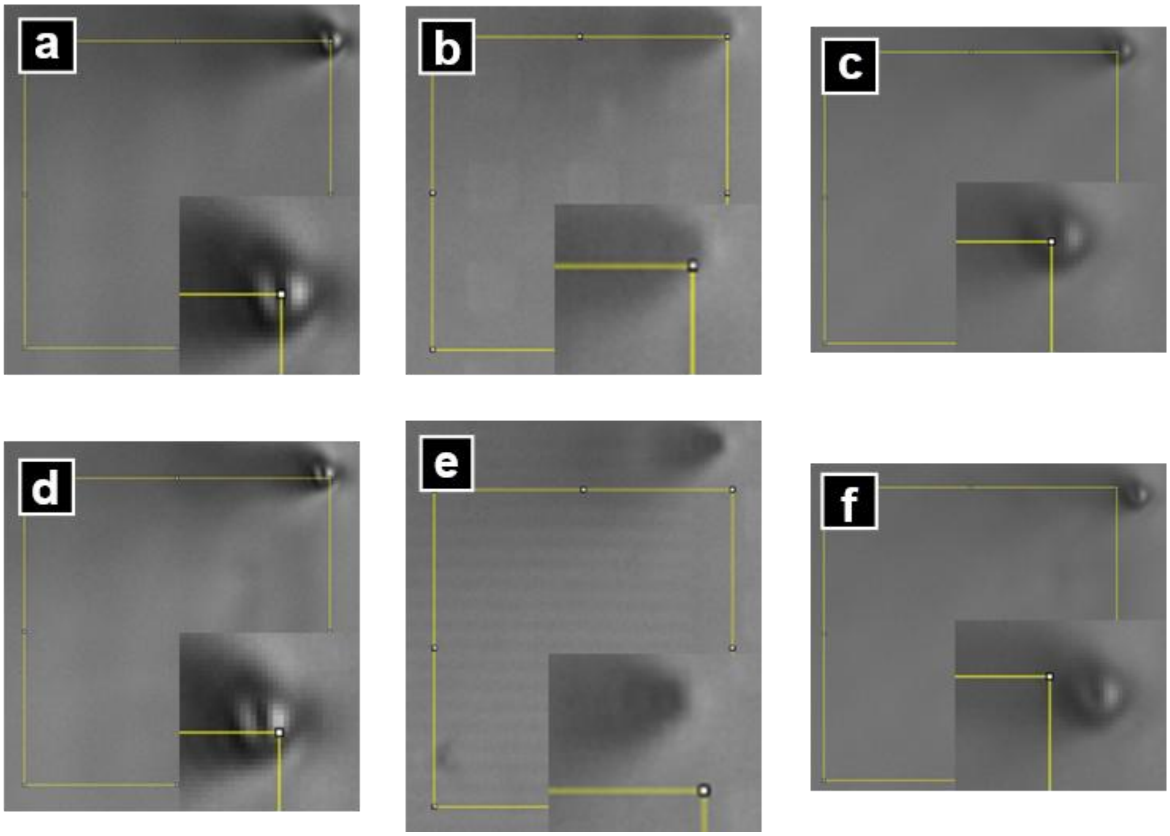

Figure S8: Optical microscopy micrographs. In the images found within this figure are the scan area seen as a yellow square (dimensions that are 30 μm x 30 μm) taken before the topography scan had been initiated for the commercial, Phrozen and Formlabs electrode holders as (a), (b) and (c), respectively. Whereas, (d), (e) and (f) are the micrographs taken just after the scan had completed for the commercial, Phrozen and Formlabs electrode holders, respectively. The yellow square in (d), (e) and (f) have the same surface area for the scan but does have the same origin (piezeos were not reset to scan origin prior to taking the after scan optical micrographs) which is why in (e) there are appear to be horizontal lines indicating a different part of the standard cast sample. All images have insets that magnify the tip position relative to the top left corner of the yellow square (aligned position for scanning). Upon scan completion the tip should not move from the drawn square, if it does then drift caused the distance seen when comparing the before and after images of each scan. Each scan took approximately 50 minutes and resulting lateral drift were estimated with ImageJ FIJI by obtaining the quantified displacement of the probe from the corner over the amount of time the scan required for data collection. This yielded the absolute drift values of 0.2, 1.2 and 0.7 nm/s for the commercial, Phrozen and Formlabs electrode holders, respectively.

S9. List of .STL Files Included in Additional SI Files

1. centrifuge_holder_body.stl
2. centrifuge_holder_screw_cap.stl
3. microelectrode_holder_sb_body_no_port.stl
4. microelectrode_holder_sb_body_thread_port.stl
5. microelectrode_holder_sb_body_with_port.stl
6. microelectrode_holder_screw_cap.stl
7. microelectrode_holder_theta_body_no_port.stl
8. microelectrode_holder_theta_body_thread_port.stl
9. microelectrode_holder_theta_body_with_port.stl

References

1 K. Alanis, Z. S. Siwy and L. A. Baker, *J. Electrochem. Soc.*, 2023, **170**, 066510.